

It consumes 24 mA from a 1.2-V supply and has a 9-GHz 3-dB bandwidth.

ACKNOWLEDGMENTS

This work was supported by the Science and Engineering Research Council of A*STAR (Agency for Science, Technology and Research), Singapore under HOME 2015 Grant.

REFERENCES

1. N. Zhang, C.-M. Hung, and K.O. Kenneth, 80-GHz tuned amplifier in bulk CMOS, *IEEE Microwave Wireless Comp Lett* 18 (2008), 121–123.
2. C. Weyers, P. Mayr, J.W. Kunze, and U. Langmann, A 22.3 dB voltage gain 6.1 dB NF 60 GHz LNA in 65 nm CMOS with differential output, *ISSCC Dig Tech Papers* (2008), 192–193.
3. T. Yao, M.Q. Gordon, K.K.W. Tang, K.H.K. Yau, M.-T. Yang, P. Schvan, and S.P. Voinigescu, Algorithmic design of CMOS LNAs and PAs for 60-GHz radio, *IEEE J Solid-State Circuits* 42 (2007), 1044–1057.
4. S.K. Reynolds, B.A. Floyd, U.R. Pfeiffer, T. Beukema, J. Grzyb, C. Haymes, B. Gaucher, and M. Soyuer, A silicon 60-GHz receiver and transmitter chipset for broadband communications, *IEEE J Solid-State Circuits* 41 (2006), 2820–2831.
5. B.A. Floyd, S.K. Reynolds, U.R. Pfeiffer, T. Zwick, T. Beukema, and B. Gaucher, SiGe bipolar transceiver circuits operating at 60 GHz, *IEEE J Solid-State Circuits* 40 (2005), 156–167.
6. S. Emami, C.H. Doan, A.M. Niknejad, and R.W. Brodersen, A highly integrated 60 GHz CMOS front-end receiver, *ISSCC Dig Tech Papers* (2007), 190–191.
7. C.-S. Wang, J.-W. Huang, S.-H. Wen, S.-H. Yeh, and C.-K. Wang, A CMOS RF front-end with on-chip antenna for V-band broadband wireless communications, *ESSCIRC Dig Tech Papers* (2007), 143–146.
8. S. Pellerano, Y. Palaskas, and K. Soumyanath, A 64 GHz 6.5 dB NF 15.5 dB gain LNA in 90 nm CMOS, *ESSCIRC Dig Tech Papers* (2007), 352–355.
9. J. Brinkhoff, K.S.S. Koh, K. Kang, and F. Lin, Scalable transmission line and inductor models for CMOS millimeter-wave design, *IEEE Trans Microwave Theory Tech* 56 (2008), 2954–2962.
10. C.H. Doan, S. Emami, A.M. Niknejad, and R.W. Brodersen, Millimeter-wave CMOS design, *IEEE J Solid-State Circuits* 40 (2005), 144–155.
11. Agilent Technologies, Advanced model composer, Agilent Technologies, Palo Alto, CA, Sep. 2006.
12. Agilent Technologies, Noise figure measurement accuracy—The Y-factor method, Application Note 57-2 [On-line], Palo Alto, CA.

© 2010 Wiley Periodicals, Inc.

BANDWIDTH ENHANCEMENT OF COUPLED-FED ON-BOARD PRINTED PIFA USING BYPASS RADIATING STRIP FOR EIGHT-BAND LTE/WWAN SLIM MOBILE PHONE

Shu-Chuan Chen and Kin-Lu Wong

Department of Electrical Engineering, National Sun Yat-sen University, Kaohsiung 80424, Taiwan; Corresponding author: chensc@ema.ee.nsysu.edu.tw

Received 30 November 2009

ABSTRACT: By connecting a bypass radiating strip to the radiating portion of a coupled-fed on-board printed PIFA (planar inverted-F antenna), significant bandwidth enhancement can be obtained. The

bypass radiating strip provides a bypass for the excited surface currents of the printed PIFA, which leads to more uniform surface current distributions on the printed PIFA. This behavior can result in slow variations in the antenna's input impedance over the operating bands, which makes it very promising to achieve improved impedance matching; thus, enhanced bandwidths of the printed PIFA are obtained. In this study, with a small footprint to be printed on the no-ground portion of $15 \times 48 \text{ mm}^2$ in the system circuit board of the mobile phone, the proposed on-board printed antenna is especially suitable for slim mobile phone applications and can generate two wide operating bands to respectively cover the LTE700/GSM850/900 operation (698–960 MHz) and the GSM1800/1900/UMTS/LTE2300/2500 operation (1710–2690 MHz). The proposed antenna held by the user's hand and attached to the user's head is also tested for its SAR values over the eight operating bands. Measured and simulated results are presented. © 2010 Wiley Periodicals, Inc. *Microwave Opt Technol Lett* 52: 2059–2065, 2010; Published online in Wiley InterScience (www.interscience.wiley.com). DOI 10.1002/mop.25406

Key words: mobile antenna; handset antenna; printed antenna; coupled-fed PIFA; bandwidth enhancement

1. INTRODUCTION

The internal antennas that can be directly printed on the system circuit board are easy to fabricate at low cost; moreover, as such on-board printed internal antennas show negligible thickness above the circuit board, they are very suitable for slim mobile phone applications [1–5]. Promising on-board printed antennas with a small printed area on the system circuit board for WWAN (wireless wide area network) operation covering the GSM850/900 bands (824–960 MHz) and GSM1800/1900/UMTS bands (1710–2170 MHz) in the mobile phone have also been reported very recently [6–24]. These on-board printed WWAN antennas include using the $\lambda/8$ printed PIFA (planar inverted-F antennas) [6], $\lambda/8$ printed monopole [11, 12], $\lambda/4$ printed slot [15–18], and $\lambda/4$ printed loop [22–24] to achieve reduced antenna size yet wide operating bands.

Among the reported on-board printed antennas, the small size and wideband operation for the printed PIFA are obtained using the coupling feed [25–27], which can result in improved impedance matching for the antenna, mainly in the 900 MHz band, to achieve a wide lower band to cover the GSM850/900 operation. This behavior on lower-band bandwidth enhancement is a significant advantage over the traditional PIFA using a direct feed [25, 28]. For the upper-band bandwidth, however, the bandwidth enhancement is not significant by using the coupling feed alone for the coupled-fed printed PIFA.

In this article, we present a coupled-fed on-board printed PIFA with a bypass radiating strip connected to the antenna's radiating portion to achieve a very wide upper band as well as a wide lower band. The bypass radiating strip does not increase the occupied size of the printed PIFA, and the obtained wide lower and upper bands can respectively cover the LTE700/GSM850/900 operation (698–960 MHz) and the GSM1800/1900/UMTS/LTE2300/2500 operation (1710–2690 MHz). That is, an eight-band LTE/WWAN on-board printed antenna for slim mobile phone applications can be obtained. Notice that the LTE operation in the 700, 2300, and 2500 MHz bands are recently introduced [29], which can provide better mobile broadband and multimedia services than the existing GSM and UMTS mobile networks [28] and will become very attractive for the mobile users. It is hence expected that the eight-band LTE/WWAN operation for the mobile phone will be demanded in the near future. In the study, effects of the bypass radiating strip on the bandwidth enhancement of the proposed on-board

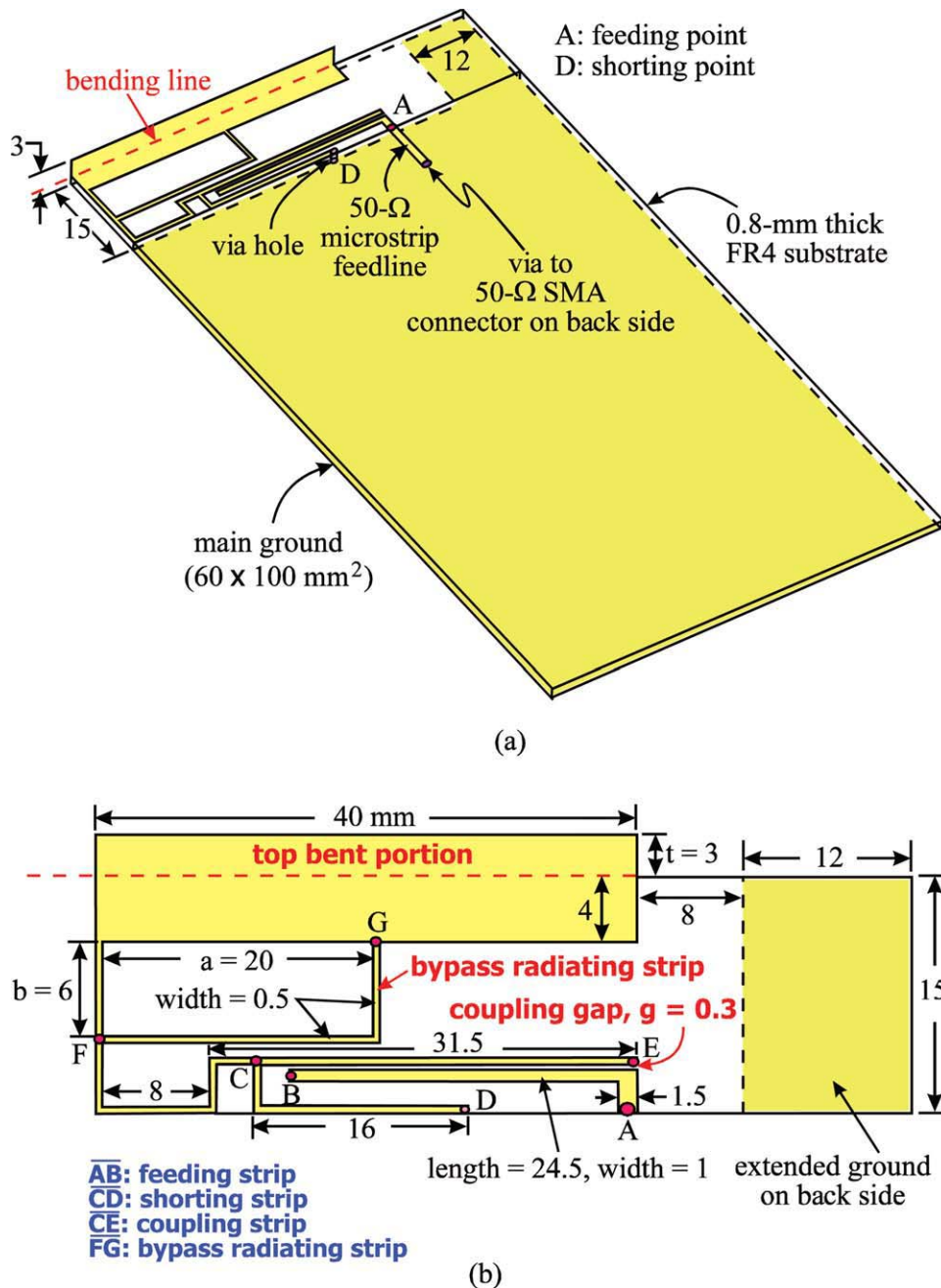


Figure 1 (a) Geometry of the proposed on-board printed PIFA using a bypass radiating strip for bandwidth enhancement to cover eight-band LTE/GSM/UMTS in the slim mobile phone. (b) Dimensions of the printed PIFA. [Color figure can be viewed in the online issue, which is available at www.interscience.wiley.com]

printed PIFA are analyzed. The radiation characteristics including the SAR (specific absorption rate) values [30–32] of the proposed antenna held by the user's hand and attached to the user's head are also studied.

2. PROPOSED ANTENNA

Figure 1(a) shows the geometry of the proposed on-board printed PIFA using a bypass radiating strip for bandwidth enhancement to cover eight-band LTE/GSM/UMTS in the slim mobile phone. Detailed dimensions of the printed PIFA are given in Figure 1(b). Notice that in Figure 1, the mobile phone housing is not considered; in this case, a top bent portion (size 3 × 40 mm²) is added in the antenna's radiating arm to lead to some impedance matching improvement in the antenna's lower band (see the results

shown in Figure 8). With the presence of a plastic mobile phone housing (relative permittivity 3.0 and conductivity 0.01 S/m) as shown in Figure 8(a), the proposed printed PIFA without the top bent portion shows similar return-loss results as that of the printed PIFA with the top bent portion shown in Figure 1. This indicates that for practical mobile phone applications, the proposed antenna can be with an all-printed structure on the system circuit board of the mobile phone.

The proposed PIFA is printed on a no-ground portion (size 15 × 48 mm²) on the 0.8-mm thick FR4 substrate (size 110 × 60 mm², relative permittivity 4.4, loss tangent 0.024), which is treated as the system circuit board of the mobile phone. On its back side, a system ground plane is printed and comprises a main ground (size 100 × 60 mm²) and an extended ground (size

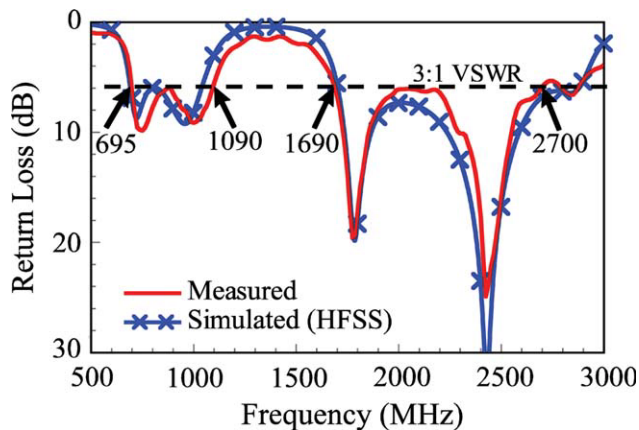


Figure 2 Measured and simulated return loss for the proposed printed PIFA. [Color figure can be viewed in the online issue, which is available at www.interscience.wiley.com]

$12 \times 15 \text{ mm}^2$). The printed PIFA is short-circuited to the main ground through the shorting strip (section CD) and uses a coupling feed, which consists of a feeding strip (section AB) and a

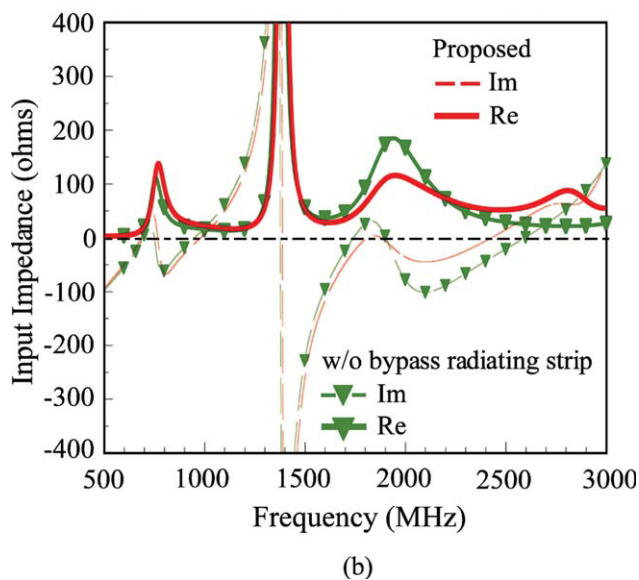
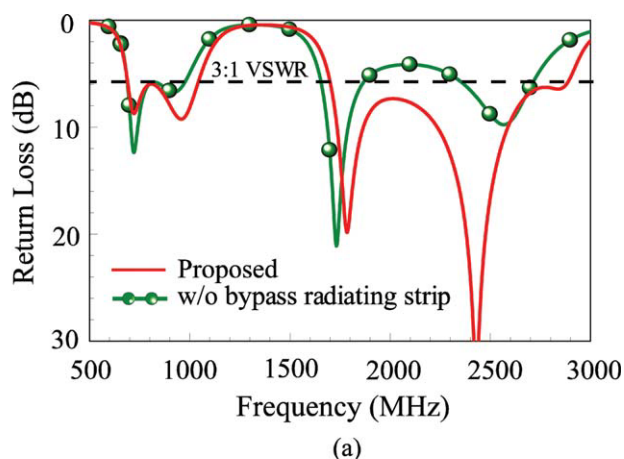


Figure 3 Comparison of (a) the simulated return loss and (b) the simulated input impedance of the proposed antenna and the case without the bypass matching strip. [Color figure can be viewed in the online issue, which is available at www.interscience.wiley.com]

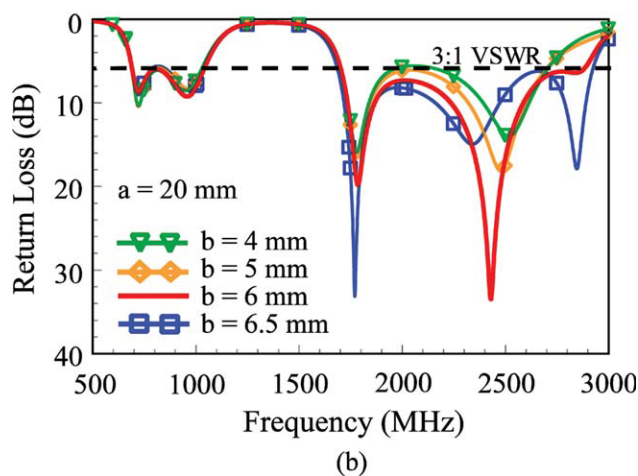
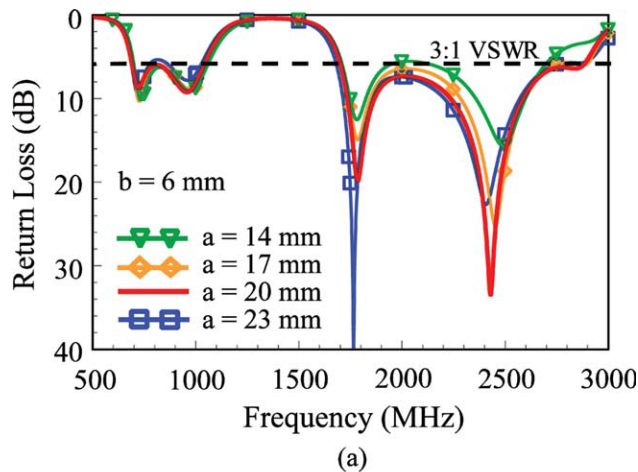


Figure 4 Simulated return loss as a function of (a) the length a and (b) the length b of the bypass radiating strip. Other dimensions are the same as given in Figure 1. [Color figure can be viewed in the online issue, which is available at www.interscience.wiley.com]

coupling strip (section CE), both separated by a coupling gap (g) of 0.3 mm. The front end of the feeding strip is at point A, which is connected to a 50- Ω microstrip feedline of short length (about 20 mm) printed on the front side of the circuit board to test the fabricated antenna in the experiment. The use of the

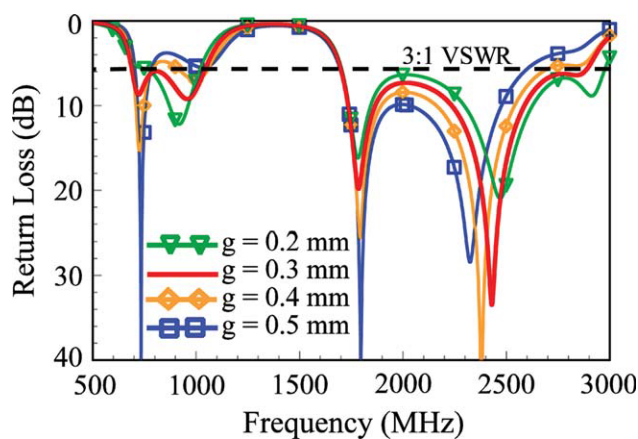


Figure 5 Simulated return loss as a function of the coupling gap g in the coupling feed. Other dimensions are the same as given in Figure 1. [Color figure can be viewed in the online issue, which is available at www.interscience.wiley.com]

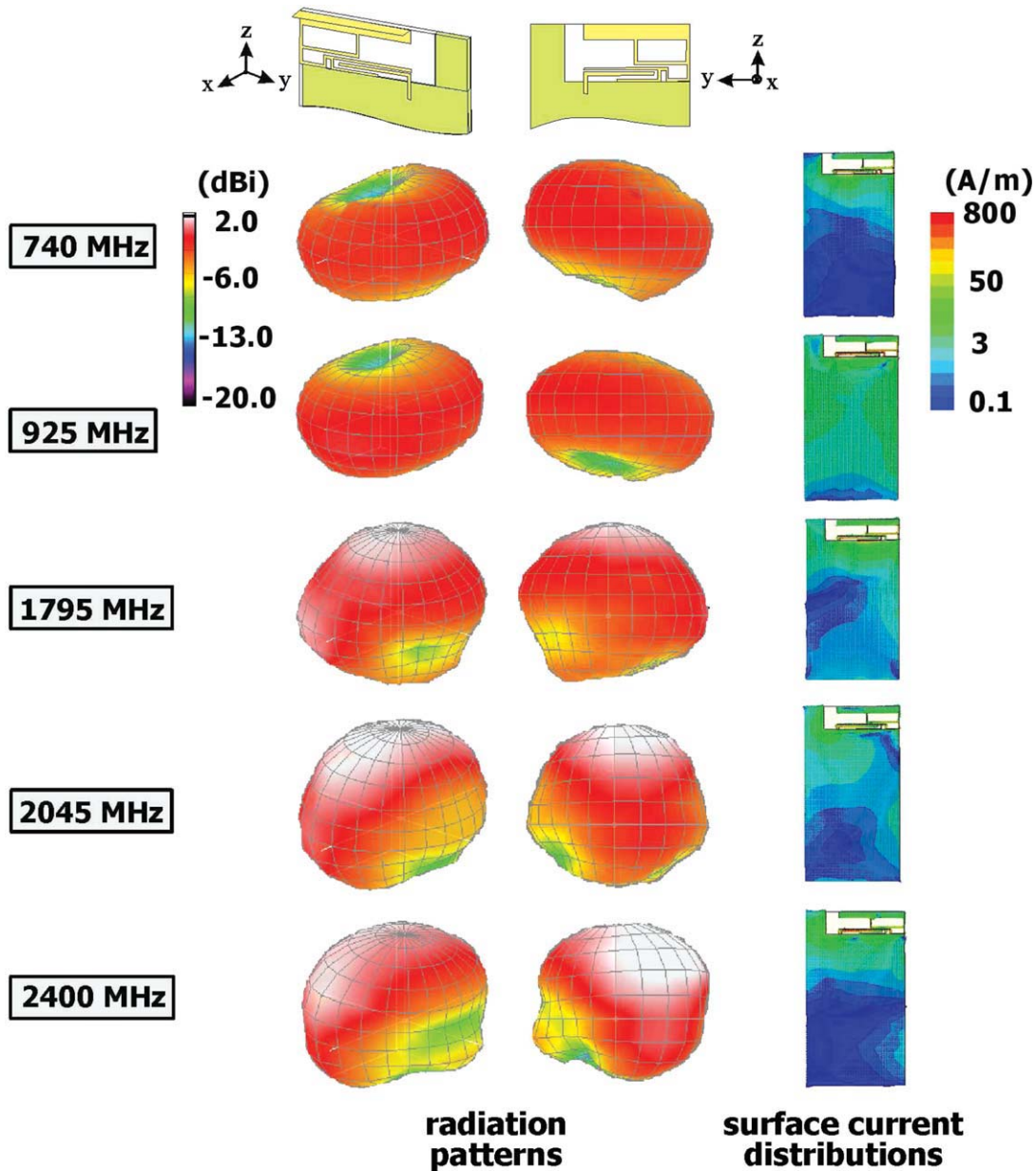


Figure 6 Measured three-dimensional (3-D) radiation patterns for the proposed antenna and simulated surface current distributions on the system ground plane. [Color figure can be viewed in the online issue, which is available at www.interscience.wiley.com]

coupling feed can lead to dual resonance in the antenna's 900 MHz band to achieve a wide lower band to cover the GSM850/900 operation (824–960 MHz) [7] or LTE700/GSM850/900 operation (698–960 MHz) in the proposed design, whose detailed operating principle has been documented in [25–27]. However, without the bypass radiating strip (section FG), this kind of coupled-fed PIFA with a single radiating strip is difficult to have a wide upper band as shown in Figure 3(a).

In the proposed antenna, the simple bypass radiating strip of length 26 mm ($a + b$ in the figure) provides a bypass for the excited surface currents on the antenna's radiating arm, which leads to more uniform excited surface current distributions. This behavior results in slow variations in the antenna's input impedance over the operating bands, especially over the antenna's upper band. This results in improved impedance matching for frequencies over the antenna's upper band. A large bandwidth of about 1 GHz (from about 1.7 to 2.7 GHz) can hence be

obtained for the antenna's upper band to cover the GSM1800/1900/UMTS/LTE2300/2500 operation (1710–2690 MHz). With the dimensions given in Figure 1, the proposed antenna is fabricated and tested.

3. RESULTS AND DISCUSSION

Figure 2 shows the measured and simulated return loss for the proposed printed PIFA shown in Figure 1. The simulated results are obtained using the simulation software HFSS version 12 [33]. The measured data agree well with the simulated results. Two wide operating bands are obtained. The antenna's lower and upper bands have respectively larger bandwidths, based on 3:1 VSWR widely used in practical mobile phone applications, of 395 MHz (695–1090 MHz) and 1010 MHz (1690–2700 MHz). This allows the proposed antenna to cover the eight-band LTE/WWAN operation.

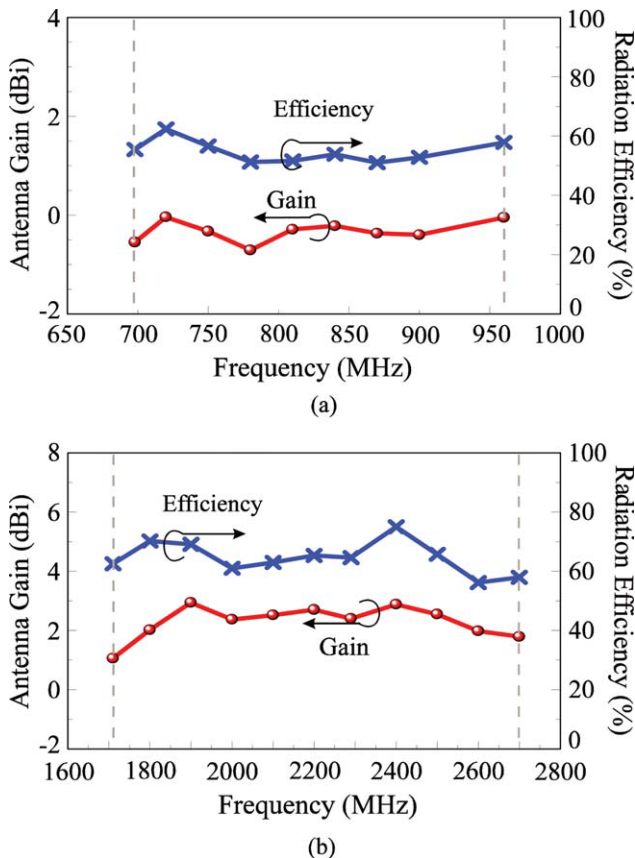


Figure 7 Measured antenna gain and radiation efficiency for the proposed antenna. (a) The lower band. (b) The upper band. [Color figure can be viewed in the online issue, which is available at www.interscience.wiley.com]

Figure 3 shows the comparison of the simulated return loss and input impedance of the proposed antenna and the case without the bypass matching strip. As seen in Figure 3(b), the variations in the real and imaginary parts of the input impedance for frequencies over the desired upper band become smaller for the proposed antenna in which the bypass radiating strip is added. This leads to significant improvement in the impedance matching seen in Figure 3(a), and a much larger bandwidth for the antenna's upper band is thus obtained. In addition, the presence of the bypass radiating strip also leads to improved impedance matching over the antenna's lower band, and a wider lower-band bandwidth is obtained.

A parametric study of the bypass radiating strip is also conducted. Figure 4 shows the simulated return loss as a function of the length a and b of the bypass radiating strip. Other dimensions are the same as given in Figure 1. In Figure 4(a), the results indicate that the length a should be larger than 14 mm such that acceptable impedance matching (3:1 VSWR) over the desired upper band can be obtained. While in Figure 4(b), it is shown that the length b should be larger than 4 mm to meet the 3:1 VSWR impedance matching over the desired upper band. From these obtained results, it can be concluded that the total length ($a + b$) of the bypass radiating strip should be at least 20 mm in the proposed antenna. Also, relatively very small variations in the impedance matching for frequencies over the lower band are seen in Figure 4(a) and 4(b).

Effects of the coupling gap between the coupling strip and feeding strip are also analyzed. Figure 5 shows the simulated return loss for the coupling gap g varied from 0.2 to 0.5 mm.

When larger coupling gaps ($g = 0.4$ and 0.5 mm) are used, significant effects on the impedance matching over the lower band are seen; in this case, the obtained lower-band bandwidth is quickly decreased. Also, for the upper band, the upper-edge frequency with 3:1 VSWR is also quickly decreased for the cases of $g = 0.4$ and 0.5 mm. When the coupling gap is too small ($g = 0.2$ mm), good excitation of the resonant mode at about 730 MHz in the lower band cannot be obtained. Based on the obtained results in Figure 5, the coupling gap in the proposed antenna is selected to be 0.3 mm.

Figure 6 shows the measured three-dimensional (3-D) radiation patterns for the proposed antenna and the simulated surface current distributions on the system ground plane. At lower frequencies (740 and 925 MHz), omnidirectional or near-omnidirectional radiation in the azimuthal plane (x - y plane) is obtained for the proposed antenna; this is owing to the domination of the excited surface currents on the system ground plane of the mobile phone in the radiation. Whereas at higher frequencies (1795, 2045, and 2400 MHz), dip or null radiation in the

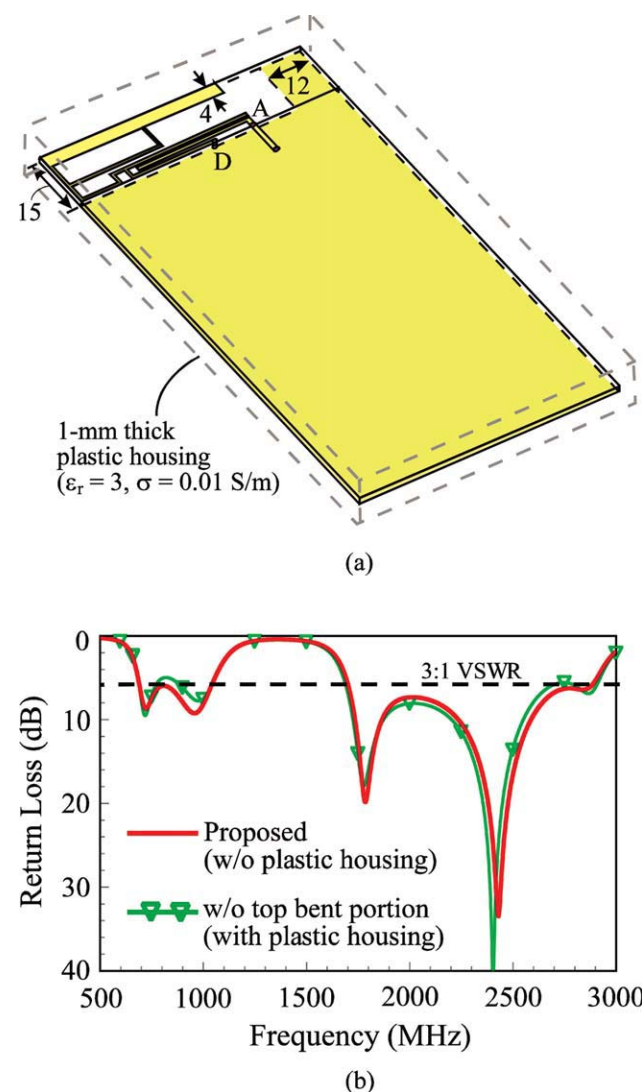
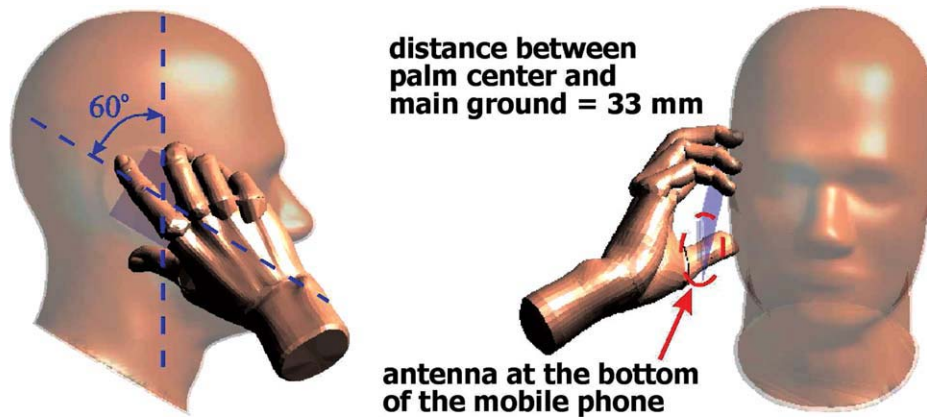


Figure 8 (a) Geometry of the proposed antenna without the top bent portion and enclosed by a 1-mm thick plastic mobile phone housing. (b) Comparison of the simulated return loss for the proposed antenna (without a plastic housing) and the case without the top bent section (with a plastic housing). [Color figure can be viewed in the online issue, which is available at www.interscience.wiley.com]



Frequency (MHz)		740	859	925	1795	1920	2045	2350	2595
1-g SAR (W/kg)	head only	0.42	1.01	1.15	0.26	0.19	0.16	0.24	0.22
	head and hand	0.42	1.01	1.16	0.60	0.60	0.53	0.62	0.82
Return loss (dB)	head only	9.2	8.4	9.9	8.3	5.1	5.6	13.6	9.4
	head and hand	11.2	7.4	8.9	12.4	5.7	4.7	9.7	8.0

Figure 9 SAR simulation model (SEMCAD [34]) and the simulated SAR values for 1-g head/hand tissue for the proposed antenna. The return loss given in the table shows the impedance matching level at the testing frequency. [Color figure can be viewed in the online issue, which is available at www.interscience.wiley.com]

azimuthal direction is seen. This is related to the nulls of the excited surface currents seen at about the center of the system ground plane.

Figure 7 shows the measured antenna gain and radiation efficiency for the proposed antenna. Measured results for the lower and upper bands are respectively shown in Figure 7(a) and 7(b). The radiation efficiency is all better than 50% for frequencies over all the operating bands. The antenna gain is about -0.7 to 0 dBi over the lower band and about 1.0 – 3.0 dBi over the upper band. The radiation performances are acceptable for practical mobile phone applications.

Notice that the proposed antenna shown in Figure 1 is without the mobile phone housing. The condition for practical applications with the mobile phone housing is studied in Figure 8. The geometry of the proposed antenna without the top bent portion and enclosed by a 1-mm thick plastic mobile phone housing is shown in Figure 8(a). The housing in the study is made of plastic materials of relative permittivity 3.0 and conductivity 0.01 S/m. The comparison of the simulated return loss for the proposed antenna (without a plastic housing) and the case without the top bent section (with a plastic housing) is presented in Figure 8(b). It can be seen that when the mobile phone housing is present, the top bent portion used for bandwidth enhancement of the proposed antenna is not necessary. This indicates that the geometry of the proposed antenna shown in Figure 1 can be further simplified and become an all-printed structure for practical applications. In this case, the proposed on-board printed PIFA is especially suitable for thin mobile phone applications.

The SAR values of the proposed antenna are also tested using SEMCAD X version 14 [34]. Both the effects of the user's head and hand are considered. The simulation SAR model with the proposed antenna held by the user's hand and attached to the user's head is shown in Figure 9. Notice that the proposed antenna is

mounted at the bottom of the mobile phone [7, 12, 20, 23] for its promising practical applications with decreased SAR values. The distance between the palm center and main ground plane of the mobile phone is set to 33 mm [31]. The obtained SAR values are tested using input power of 24 dBm for GSM850/900 operation (859, 925 MHz) and 21 dBm for GSM1800/1900 operation (1795, 1920 MHz), UMTS operation (2045 MHz) and LTE operation (740, 2350, 2595 MHz); the results are given in the figure. The return loss given in the figure shows the impedance matching level at the testing frequency when only the user's head is present or both the user's head and hand are present. Results show that the SAR values for the cases with and without the user's hand are about the same over the lower band. Conversely, much larger SAR values owing to the presence of the user's hand are seen over the upper band. However, it is observed that over the eight operating bands, the obtained SAR values are all well below the SAR limit of 1.6 W/kg for the 1.0-g head/hand tissue [30]. The results suggest that the proposed antenna is promising for practical mobile phone applications.

4. CONCLUSION

An on-board printed PIFA with small size yet large operating bandwidths in both its lower and upper bands has been proposed and studied. The wide lower band is mainly owing to the use of the coupling feed, whereas the wide upper band is owing to the use of the bypass radiating strip. The obtained bandwidths of the antenna's lower and upper bands are respectively larger than 698–960 MHz and 1710–2690 MHz, allowing the proposed antenna very promising to cover the eight-band LTE/WWAN operation. Good radiation characteristics for frequencies over the eight operating bands have also been observed. The obtained SAR values considering both the user's head and hand are found to be well below 1.6 W/kg for 1-g tissue. From the obtained

results, the proposed antenna is very suitable for practical applications, especially in the slim mobile phones.

REFERENCES

1. K.L. Wong, Y.C. Lin, and T.C. Tseng, Thin internal GSM/DCS patch antenna for a portable mobile terminal, *IEEE Trans Antennas Propag* 54 (2006), 238–242.
2. K.L. Wong, Y.C. Lin, and B. Chen, Internal patch antenna with a thin air-layer substrate for GSM/DCS operation in a PDA phone, *IEEE Trans Antennas Propag* 55 (2007), 1165–1172.
3. R.A. Bhatti and S.O. Park, Hepta-band internal antenna for personal communication handsets, *IEEE Trans Antennas Propag* 55 (2007), 3398–3402.
4. R.A. Bhatti, Y.T. Im, J.H. Choi, T.D. Manh, and S.O. Park, Ultrathin planar inverted-F antenna for multistandard handsets, *Microwave Opt Technol Lett* 50 (2008), 2894–2897.
5. H. Rhyu, J. Byun, F.J. Harackiewicz, M.J. Park, K. Jung, D. Kim, N. Kim, T. Kim, and B. Lee, Multi-band hybrid antenna for ultrathin mobile phone applications, *Electron Lett* 45 (2009), 773–774.
6. C.H. Chang and K.L. Wong, Printed $\lambda/8$ -PIFA for penta-band WWAN operation in the mobile phone, *IEEE Trans Antennas Propag* 57 (2009), 1373–1381.
7. C.T. Lee and K.L. Wong, Uniplanar coupled-fed printed PIFA for WWAN/ WLAN operation in the mobile phone, *Microwave Opt Technol Lett* 51 (2009), 1250–1257.
8. J.H. Kim, W.W. Cho, and W.S. Park, A small printed dual-band antenna for mobile handsets, *Microwave Opt Technol Lett* 51 (2009), 1699–1702.
9. H.W. Hsieh, Y.C. Lee, K.K. Tiong, and J.S. Sun, Design of a multiband antenna for mobile handset operations, *IEEE Antennas Wireless Propag Lett* 8 (2009), 200–203.
10. T.W. Kang and K.L. Wong, Simple small-size coupled-fed uniplanar PIFA for multiband clamshell mobile phone application, *Microwave Opt Technol Lett* 51 (2009), 2805–2810.
11. T.W. Kang and K.L. Wong, Chip-inductor-embedded small-size printed strip monopole for WWAN operation in the mobile phone, *Microwave Opt Technol Lett* 51 (2009), 966–971.
12. C.H. Chang and K.L. Wong, Small-size printed monopole with a printed distributed inductor for penta-band WWAN mobile phone application, *Microwave Opt Technol Lett* 51 (2009), 2903–2908.
13. K.L. Wong and T.W. Kang, GSM850/900/1800/1900/UMTS printed monopole antenna for mobile phone application, *Microwave Opt Technol Lett* 50 (2008), 3192–3198.
14. K.L. Wong, Y.W. Chi, and S.Y. Tu, Internal multiband printed folded slot antenna for mobile phone application, *Microwave Opt Technol Lett* 49 (2007), 1833–1837.
15. C.I. Lin and K.L. Wong, Printed monopole slot antenna for internal multiband mobile phone antenna, *IEEE Trans Antennas Propag* 55 (2007), 3690–3697.
16. C.H. Wu and K.L. Wong, Hexa-band internal printed slot antenna for mobile phone application, *Microwave Opt Technol Lett* 50 (2008), 35–38.
17. C.I. Lin and K.L. Wong, Printed monopole slot antenna for penta-band operation in the folder-type mobile phone, *Microwave Opt Technol Lett* 50 (2008), 2237–2241.
18. F.H. Chu and K.L. Wong, Simple folded monopole slot antenna for penta-band clamshell mobile phone application, *IEEE Trans Antennas Propag* 57 (2009), 3680–3684.
19. Y.W. Chi and K.L. Wong, Internal compact dual-band printed loop antenna for mobile phone application, *IEEE Trans Antennas Propag* 55 (2007), 1457–1462.
20. K.L. Wong and W.Y. Chen, Small-size printed loop antenna for penta-band thin-profile mobile phone application, *Microwave Opt Technol Lett* 51 (2009), 1512–1517.
21. W.Y. Li and K.L. Wong, Internal printed loop-type mobile phone antenna for penta-band operation, *Microwave Opt Technol Lett* 49 (2007), 2595–2599.
22. Y.W. Chi and K.L. Wong, Very-small-size printed loop antenna for GSM/DCS/PCS/UMTS operation in the mobile phone, *Microwave Opt Technol Lett* 51 (2009), 184–192.
23. Y.W. Chi and K.L. Wong, Quarter-wavelength printed loop antenna with an internal printed matching circuit for GSM/DCS/PCS/UMTS operation in the mobile phone, *IEEE Trans Antennas Propag* 57 (2009), 2541–2547.
24. Y.W. Chi and K.L. Wong, Very-small-size folded loop antenna with a band-stop matching circuit for WWAN operation in the mobile phone, *Microwave Opt Technol Lett* 51 (2009), 808–814.
25. K.L. Wong and C.H. Huang, Bandwidth-enhanced internal PIFA with a coupling feed for quad-band operation in the mobile phone, *Microwave Opt Technol Lett* 50 (2008), 683–687.
26. K.L. Wong and C.H. Huang, Compact multiband PIFA with a coupling feed for internal mobile phone antenna, *Microwave Opt Technol Lett* 50 (2008), 2487–2491.
27. K.L. Wong and C.H. Huang, Printed PIFA with a coplanar coupling feed for penta-band operation in the mobile phone, *Microwave Opt Technol Lett* 50 (2008), 3181–3186.
28. K.L. Wong, *Planar antennas for wireless communications*, Wiley, New York, 2003.
29. S. Sesia, I. Toufik, and M. Baker (Eds), *LTE, The UMTS long term evolution: from theory to practice*, Wiley, New York, 2009.
30. Safety levels with respect to human exposure to radio-frequency electromagnetic field, 3 kHz to 300 GHz, ANSI/IEEE standard C95.1, American National Standards Institute (ANSI), Boulder, CO, 1999.
31. C. H. Li, E. Ofli, N. Chavannes, and N. Kuster, Effects of hand phantom on mobile phone antenna performance, *IEEE Trans Antennas Propag* 57 (2009), 2763–2770.
32. J.C. Lin, Specific absorption rates induced in head tissues by microwave radiation from cell phones, *Microwave* 40 (2001), 22–25.
33. Ansoft Corporation HFSS, Available at <http://www.ansoft.com/products/hf/hfss/>, Ansoft Corporation HFSS, Pittsburgh, PA.
34. Schmid & Partner Engineering AG (SPEAG), Available at <http://www.semcad.com>, SEMCAD, Schmid & Partner Engineering AG (SPEAG).

© 2010 Wiley Periodicals, Inc.

MICROSTRIP-FED SMALL SQUARE MONOPOLE ANTENNA FOR UWB APPLICATION WITH VARIABLE BAND-NOTCHED FUNCTION

R. Rouhi,¹ Ch. Ghobadi,¹ J. Nourinia,¹ and M. Ojaroudi²

¹ Department of Electrical Engineering, Urmia University, Urmia, Iran; Corresponding author: st_r.rouhi@urmia.ac.ir

² Department of Electrical Engineering, GBAU, Germi, Iran

Received 6 December 2009

ABSTRACT: In this article, a novel square monopole antenna for ultra wideband applications with variable frequency band-notch characteristic is presented. By using T-shaped slots, additional resonances are excited and hence, the fractional bandwidth is increased up to 150%. A modified T-shaped conductor-backed plane is used to generate the frequency band-stop performance. © 2010 Wiley Periodicals, Inc. *Microwave Opt Technol Lett* 52: 2065–2069, 2010; Published online in Wiley InterScience (www.interscience.wiley.com). DOI 10.1002/mop.25395

Key words: monopole antenna

1. INTRODUCTION

Commercial ultra wideband (UWB) systems require small low-cost antennas with omnidirectional radiation patterns and large bandwidth [1]. It is a well-known fact that planar monopole antennas present really appealing physical features, such as simple structure, small size, and low cost. Due to all these